Proceedings of the ASME 2010 3rd Joint US-European Fluids Engineering Summer Meeting and 8th International Conference on Nanochannels, Microchannels, and Minichannels
FEDSM-ICNMM2010
August 1-5, 2010, Montreal, Canada

FEDSM-ICNMM2010-30177

NEUTROPHIL MOTION, ADHESION AND ACTIVATION IN AN *IN VITRO* MICROPIPETTE MODEL OF A LUNG CAPILLARY

David F. J. Tees
Dept. of Physics & Astronomy
Ohio Unversity
Athens, OH, USA

Prithu Sundd
La Jolla Institute of
Allergy & Immunology
La Jolla, CA, USA

Young Eun Choi
Dept. of Physics & Astronomy
Ohio University
Athens, OH, USA

Douglas J. Goetz
Dept. of Chem. & Biomol. Eng.,
Ohio University
Athens, OH, USA

Anand Pai
Dept. of Biomed. Eng.,
Duke University
Durham, NC, USA

Steven Rogers
Dept. of Physics & Astronomy
Ohio University
Athens, OH, USA

ABSTRACT

White blood cell (WBC) sequestration in lung capillaries is a key step in the inflammatory response to lung infection. P-selectin and ICAM-1 have well-defined roles in WBC adhesion in venules but their role in pulmonary capillaries is still unclear. Here, a novel *in vitro* Micropipette Cell Adhesion Assay used P-selectin, ICAM-1 or BSA-coated capillary-sized glass micropipettes as an in vitro model of a lung capillary. WBC were aspirated into adhesion molecule-coated vessels of varying diameters. Cell velocities and activation times were determined under pressures representative of lung capillaries. WBC velocities in this assay were significantly lower on P-selectin than BSA and decreased with increasing P-selectin concentration. These results demonstrate that P-selectin at low density mediates WBC adhesion in the pulmonary capillary geometry. WBC can also become activated upon aspiration into micropipettes and under some circumstances can be seen to exhibit a cyclic migratory behavior. This work was supported by grant BES-0547165 from the National Science Foundation and by an award from the American Heart Association.

INTRODUCTION

White blood cell (WBC) arrest in capillaries is part of the response to inflammation, sepsis and injury [1-4]. The resulting sequestration of WBC in organs with dense capillary beds, like the lung, results in a diminution of WBC elsewhere in the body [5-7]. Sequestration of WBC in capillaries has been studied in vivo, but the mechanism is still the subject of debate. WBC are typically 6-8 μm in diameter while capillaries through which they travel are only 2-8 μm in diameter [8]. As a result, WBC undergo considerable deformation entering capillaries. WBC are much less deformable than red blood cells (RBC, the vast majority of circulating blood cells) and it can take a some time for a WBC to enter the vessel. Once inside, however, the force due to the pressure difference across the cell should drive the cell at a constant velocity unless there is tapering of the vessel or adhesion between the cell and vessel wall. This constancy has been verified by Shao & Hochmuth [9].

Capillary Networks

Capillaries have different geometries and pressure drops in different tissues. In muscle, capillaries tend to be long with relatively little branching. The pressure drops across a segment can be on the order of 1000 Pa. In the liver, kidney and lung, however, capillaries form dense beds with short segments that have been modeled as open plates with occasional obstructions ("posts in a garage") [10]. As shown in Fig. 2, however, other micrographic studies [11] have shown that for the lung, it is also plausible to model the alveolar capillary bed (i.e. the bed that surrounds the alveoli where oxygen transfer takes place) as a densely interconnected network of tubules. Here, the capillary segments are short and the pressure drop across each segment is much lower (10-80 Pa) than in muscle capillaries [12, 13].

Physiological and Pathological WBC Sequestration

The lung alveoli are also places where inhaled bacteria can come into contact with sensitive tissue and thus a robust host defense by WBC is required to repel these invaders. This is the functional reason for WBC to arrest and exit the capillary beds

to fight infection from lung alveolar capillaries. In some situations, however, lung sequestration of WBC can become pathological, leading to fluid accumulation (edema) in the alvelolar air-space and to Acute Lung Injury (ALI) and Acute Respiratory Distress Syndrome (ARDS). ALI/ARDS affects ~200,000 patients in the US every year [4, 14-20] and is thus a major cause of morbidity. There is, therefore, much interest in understanding the sequestration of RBC in lung alveolar capillaries both physiologically and pathologically.

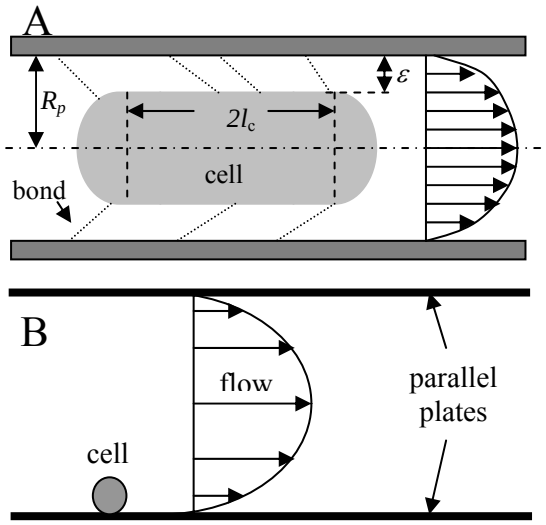

Figure 1. A) Diagram showing the variables needed to describe the forces on a capsule-shaped body moving inside a capillary at very low Reynolds number. The ligands on the surface of the cell body bind to receptors on the capillary wall resulting in a drag force.
B) Geometry of a cell in a venule or a parallel plate flow chamber. A minimally deformed spherical cell is driven along by hydrodynamic shear. Reproduced with permission from [49].

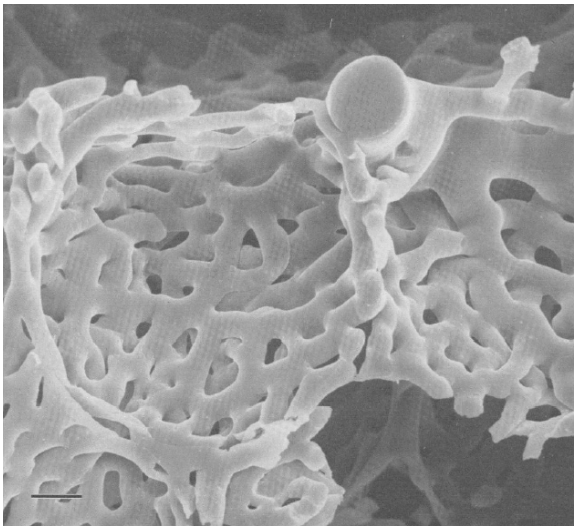

Figure 2. Micrograph of a latex cast of the rat lung alveolar capillary bed showing the interconnected network of tubules. Bar = 10 μm. Reproduced with permission from Fig. 4 of [11].

Sequestration Mechanism

Adhesion is an attractive candidate mechanism for cell arrest in capillaries. It has been amply demonstrated that WBC roll and firmly adhere to endothelial cells (EC) that line post-capillary venules [21-31]. While still considered part of the microcirculation, venules are larger than capillaries and venular EC is known to express adhesion molecules that interact with ligands on WBC [32]. The most likely mediators of adhesion in capillaries are the proteins P- and E-selectin, that are expressed on stimulated EC [33] and bind to carbohydrate-bearing glycoproteins expressed on the surfaces of WBC [34, 35]. Current *in vivo* studies, however, show that while these molecules are expressed at high levels in post-capillary venules, only levels near the threshold of detection are present in capillaries and there may be capillary tissues where they are not expressed at all. Another ligand possibility is protein ICAM-1 which is expressed on EC and binds to the integrins LFA-1 and Mac-1 on WBC [32]. In venules, WBC adhesion is a multistep process involving initial tethering and rolling (both of which are mediated primarily by selectins), followed by firm arrest and activation (mediated primarily by integrins), and finally transendothelial migration [36]. The alternate mechanism for arrest in capillaries is an ill-defined "mechanical trapping". Observations of lung EC, however, show that there can be upregulation of P-selectin in lung microvasculature following complement treatment in normal mice[1]. On the other hand, antibody blocking studies have shown that blocking β_2 integrins (that bind to ICAM-1) and P-selectin had little effect on initial sequestration, but anti-β_2 integrin antibodies and the selectin inhibitor fucoidin did affect subsequent retention [5, 7, 37]. There is also no observed change in sequestration of WBC in P/E-selectin knockout mice or in β_2 integrin knockout mice [1]. These results, however, only imply that if P-selectin and β_2 integrins are not present, there is some other mechanism that mediates arrest. The experiments do not rule out some role for adhesion molecules in arrest, if the molecules are present.

Central Hypothesis

We hypothesized that WBC arrest in capillaries involved both mechanical and biochemical adhesive forces: mechanical forces alter the area of contact between the WBC and the endothelium and thus modulate biochemical adhesive force. Because the contact area is larger and the forces from elastic shape recovery of WBC bring cell surfaces into closer contact with the capillary wall than hydrodynamic forces bring them in venules, low densities of adhesion molecules can play a role in the adhesion [4]. This additional contact should increase the rate for bond formation and generate bonds to oppose the force from the pressure drop across the cell. To sort out the role of these (and potentially other) adhesion molecules in arrest, knowledge of the behavior that would be expected for WBC in the presence of known low concentrations of ECAMs in the restricted capillary geometry is required. Use of micropipette to mimic the pulmonary capillary was seen as a good geometrical environment to observe the mechanics of WBC adhesion.

The Need for an Assay

Resolving the questions surrounding the mechanism for cell arrest in capillaries requires a well-defined geometrical and fluid mechanical environment. Micropipettes can be used to simulate the capillary geometry and it is anticipated that a "flow chamber" assay for adhesion in capillaries will prove equally valuable for unraveling cell arrest in capillaries as parallel plate flow chambers have been for rolling adhesion in larger vessels. Various sizes of non-tapering micropipettes were coated with sP-selectin to study biochemical arrest at different surface densities. BSA coated micropipettes were used as a control. The cell velocity (average and standard error) was measured to assess the dynamics of WBC adhesion under differing degrees of deformation.

NOMENCLATURE

Abbreviations:

ALI = Acute Lung Injury
ARDS = Acute Respiratory Distress Syndrome
BSA = Bovine Serum Albumin
CMB = Cyclic Migratory Behavior
EC = Endothelial Cell
ELISA = Enzyme-linked ImmunoSorbent Assay
RBC = Red Blood Cell(s)
sP-s = soluble P-selectin
WBC = White Blood Cell(s)

Symbols:

U = velocity of a tethered cell in a micropipette
U_f = velocity of an untethered cell in a micropipette
F = external force (due to bonds) acting on a cell
l_c = half length of flattened section of cell in a micropipette
L_{eq} = length of micropipette over which pressure drop occurs (excluding the length of the cell).
$\bar{L}_{eq} = L_{eq}/R_p$ = dimensionless equivalent length of micropipette
R_p = radius of micropipette
ΔP = pressure difference across micropipette system
μ = viscosity of suspending medium
$\bar{\beta} = l_c/R_p$ = ratio of flattened section length to micropipette
ε = gap width between flattened section of cell and vessel wall
$\bar{\varepsilon} = \varepsilon/R_p$ = dimensionless gap width
$\zeta = R_c/R_p$ = ratio cell diameter to micropipette diameter
Φ = Function that multiplies force in Eq. 1
Ψ = Function that multiplies velocity in Eq. 1

Subscripts:

c = cell
p = pipette

THEORY

Cell Motion and Arrest in a Small Tube

For a WBC to be at rest in a capillary there must be a balance of forces acting on it. WBC motion in a fluid filled capillary is driven by a pressure difference, ΔP, between the leading and trailing edges. Shao & Hochmuth [9] showed that for a smooth capsule-shaped body with flattened length, $2l_c$, perfectly centered in a straight tube with circular cross-section of radius R_p (see Fig. 1), the total pressure drop across the micropipette system, ΔP, is related to cell velocity inside the micropipette, U and external force on the cell (due to bonds), F:

$$\Delta P \approx U\left(\frac{\mu\Psi\left(\bar{\beta},\bar{\varepsilon},\bar{L}_{eq}\right)}{R_p}\right)+F\left(\frac{\Phi\left(\bar{\beta},\bar{\varepsilon},\bar{L}_{eq}\right)}{\pi R_p^2}\right) \quad (1)$$

Ψ and Φ are functions of dimensionless versions of the geometrical parameters shown in Fig. 1, where all parameters are scaled to the micropipette radius, R_p: the dimensionless flattened section length, $\bar{\beta} = l_c/R_p$, the dimensionless gap width, $\bar{\varepsilon} = \varepsilon/R_p$ and the dimensionless equivalent length of the micropipette, $\bar{L}_{eq} = L_{eq}/R_p$:

$$\Psi\left(\bar{\beta},\bar{\varepsilon},\bar{L}_{eq}\right)=\left(\frac{4\bar{\beta}}{\bar{\varepsilon}}+\frac{17\sqrt{2}\pi}{4\bar{\varepsilon}^{1/2}}\right)+\left(2\bar{\beta}-\frac{3\pi^2}{32\bar{\beta}}-\frac{66}{5}\right)+$$
$$8\left(\bar{L}_{eq}-2\left(1-\bar{\varepsilon}\right)-2\bar{\beta}\right)\left(1-\bar{\varepsilon}-\frac{\pi}{8\sqrt{2}}\frac{1}{\bar{\beta}}\bar{\varepsilon}^{3/2}\right) \quad (2)$$

and

$$\Phi\left(\bar{\beta},\bar{\varepsilon},\bar{L}_{eq}\right)=\left(1+\bar{\varepsilon}+\frac{\sqrt{2}\pi}{16\bar{\beta}}\bar{\varepsilon}^{3/2}\right)+$$
$$8\left(\bar{L}_{eq}-2\left(1-\bar{\varepsilon}\right)-2\bar{\beta}\right)\left(\frac{\bar{\varepsilon}^3}{\bar{\beta}}-\frac{3\pi}{8\sqrt{2}}\frac{1}{\bar{\beta}^2}\bar{\varepsilon}^{7/2}\right) \quad (3)$$

One can easily rewrite Eq. (1) to find the cell velocity as a function of the pressure drop and the external forces on the cell.

$$\frac{U}{R_p}=\left(\frac{1}{\mu\Psi\left(\bar{\beta},\bar{\varepsilon},\bar{L}_{eq}\right)}\right)\Delta P-\left(\frac{1}{\mu\pi R_p^2}\frac{\Phi\left(\bar{\beta},\bar{\varepsilon},\bar{L}_{eq}\right)}{\Psi\left(\bar{\beta},\bar{\varepsilon},\bar{L}_{eq}\right)}\right)F \quad (4)$$

If there are no bonds, then free velocity, U_f is given by:

$$U_f=\frac{R_p\Delta P}{\mu\Psi\left(\bar{\beta},\bar{\varepsilon},\bar{L}_{eq}\right)} \quad (5)$$

If the presence of bonds has no effect on the gap width (perhaps a debatable assumption, but a reasonable starting point) then we can substitute Eq. (5) into Eq. (1), to get the force exerted by the bonds in terms of the observed cell velocity (which will be less than the free velocity) and the pressure drop across the micropipette system:

$$F=\frac{\pi R_p^2\Delta P}{\Phi\left(\bar{\beta},\bar{\varepsilon},\bar{L}_{eq}\right)}\left[1-\frac{U}{U_f}\right]. \quad (6)$$

Shao and Hochmuth [38] noted that for small $\bar{\varepsilon}$, $\Phi\left(\bar{\beta},\bar{\varepsilon},\bar{L}_{eq}\right)\rightarrow 1$, so for all the work described below:

$$F=\pi R_p^2\Delta P\left(1-\frac{U}{U_f}\right) \quad (7)$$

Cell Motion in Tapering Tubes

This theory assumes that the capillary is non-tapering. There has also been work on the motion of cells in tapering tubes. In this geometry one can get mechanical arrest since curved membrane segments (that have radii of curvature R_1 and R_2) at either end of a cell in a tapering tube are maintained by the difference between the pressure inside the cell and the pressures P_1 upstream and P_2 downstream of the cell. The Law of Laplace for these two surfaces can be used to eliminate P_{cell} and show that $P_1–P_2 = 2\tau(1/R_2–1/R_1)$ where τ is the surface tension. If the curvature difference of the end caps is large enough, this pressure difference can equal the circulatory pressure difference across the cell and lead to arrest [39-44]. This theory has been expanded to model the dynamics of cell motion in a tapering vessel [45, 46]. More complex taper geometries have also been simulated [12]. Importantly, this analysis suggests that mechanical arrest requires some change in vessel diameter. Capillaries are not necessarily straight tubes and there is likely to be tapering at the enlarged "vestibules" where vessels bifurcate. Mechanical arrest has been observed both in junction regions and in straight segments (where there is little tapering) [3]. Because adhesion can occur in both regions, it is necessary to determine what type of behavior can be expected under well-characterized geometrical conditions.

Deformation Ratio (ζ)

When a spherical WBC is completely aspirated into a capillary-sized tube, it deforms into a capsule shape with radius approximately equal to the radius of the microvessel R_p. It can be easily shown that if one defines the Deformation Ratio, $\zeta = R_c/R_p$, where R_c is the radius of initially spherical cell, then the relative area of the capsule shaped cell is approximately:

$$A_{capsule}/4\pi R_c^{\,2} = \left[1+(2/3)\left(\zeta^3-1\right)\right]/\zeta^2 \qquad (8)$$

and the fraction of the total area of the capsule shaped cell that is in contact with the glass microvessel wall is:

$$A_{contact}/A_{capsule} = (2/3)\left(\zeta^3-1\right)/\left[1+(2/3)\left(\zeta^3-1\right)\right] \qquad (9)$$

MATERIALS AND METHODS

HL-60 Cells

For initial experiments to develop the system, undifferentiated HL-60 cells (a promyelocytic leukemia line) were obtained from ATCC and grown in culture [47]. Aliquots of cells were washed (by micro-centrifugation at 380G for 2 min) in plain RPMI1640 medium (maintained at 37ºC) and then suspended in $HBSS^+$ (Hanks' Balanced Salt Solution with added Ca^{2+} and Mg^{2+}, Cambrex, Walkersville, MD) with 1% BSA (A7030, Sigma) added. The average diameter of the HL-60 cells used was 13.5 ± 0.8 (SD) μm.

Neutrophils

Blood samples from healthy donors were collected by finger prick into microhematocrit tubes. Neutrophils (the most common WBC subtype) were separated from the whole blood by centrifuging the blood for 15 min at 100 G in the hematocrit tubes over an equal volume of Mono-poly Resolving Medium (M-PRM, MP Biomedicals, LLC, Solon, OH). The tubes were cut to obtain the fraction that had neutrophils and these cells were diluted into heat-treated $HBSS^+$ with 1% BSA and kept at room temperature for at least 20 min to allow the cells to go back to a resting state following the purification. Cells were used within 2-3 hours.

Adhesion Molecules

A recombinant non-chimeric form of human soluble P-selectin (sP-s) was a generous gift from Raymond T. Camphausen, Wyeth Research, Cambridge, MA. Concentrations of sP-selectin of 0.2, 0.6, 1, 10, 20, 50, and 100 μg/ml were used. ICAM-1 was purchased from R&D Systems, Inc.

Fabrication and Characterization of Glass Micropipettes

Forged glass micropipettes with inner diameters ranging from 4.5 to 8.0 μm, were fabricated using custom 0.9 mm thin-walled glass capillary tubing using a micropipette/needle puller (Model 730, David Kopf Instruments, Tujunga, CA). A microforge (MF-200, World Precision Instruments, Sarasota, FL) was used to smooth the tips of the micropipettes to ensure that the cells were not damaged during aspiration. Micropipette tip ID was measured using fine needles (also made using the Kopf puller) that had been sputter-coated with gold, and imaged using a Scanning Electron Microscope (Jeol, JSM 5300, Tokyo) to obtain a calibration curve of diameter vs insertion length. The insertion length of the needle was used to get the tip inner diameter from the calibration curve.

Coating of Micropipettes With sP-selectins

A custom holder (Fig. 3, top left) was used to coat micropipettes with adhesion molecules. Micropipettes tips were washed once with 100% ethanol, then three times with $HBSS^-$ (Hanks' Balanced Salt Solution without Ca^{2+} and Mg^{2+}, Cambrex, Walkersvile, MD). The micropipette was then coated with the diluted sP-selectin in 0.1M $NaHCO_3$, pH 9.2. The micropipette tip was dipped into sP-selectin, immediately pulled out to avoid the diffusion from the bulk solution, and then incubated for 2 min. After 2 min incubation, it was washed again with $HBSS^-$ three times. The micropipettes was transferred into the custom-made Plexi-glass stands, and filled with heat-treated $HBSS^+$+ 1% BSA (pH 7.4) until use.

The surface densities coated on the outside of the micropipettes were assayed using Enzyme Linked Immunosorbent Assay (ELISA) and found to be comparable to densities used in parallel plate flow chamber experiments. To ensure that the surface density on the inside and outside walls of the micropipette tip are comparable, micropipette tips with inner diameter = 7.5 μm were coated with FITC anti-P-Selectin antibody. Figure 3, top right, shows the averaged intensity for a cut across the micropipette. Four peaks, that represent the outer and inner walls of the two sides of the micropipette, all have comparable intensity. This implies that the surface density on the outside wall is a plausible estimate of the surface density on the inside wall.

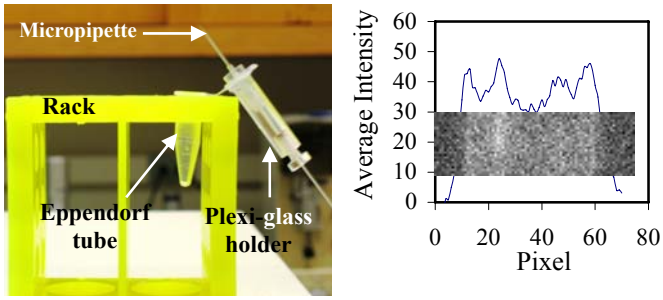

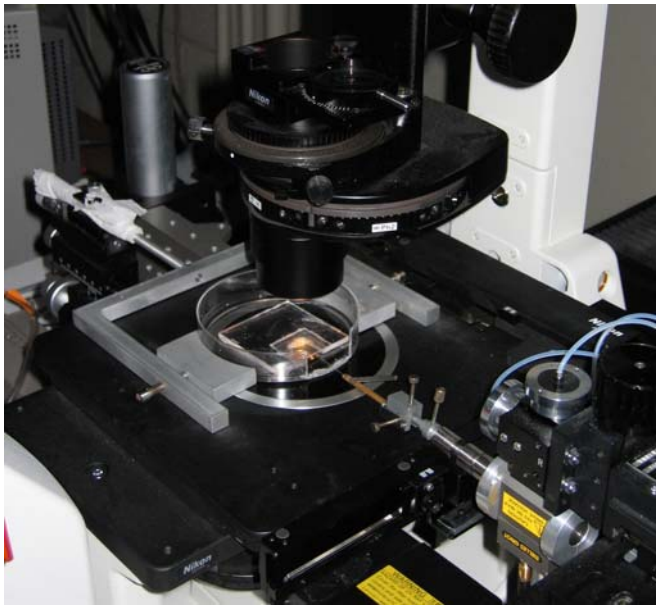

Figure 3. Top left) Holder system used for coating micropipettes with adhesion molecules. Top right) Average intensity for cuts across the fluorescently-coated micropipette that is shown overlaid on the graph. Bottom) Viewing chamber with inserted micropipette.

Micropipette cell adhesion assay and aspiration procedure

A polycarbonate insert with a 0.5 ml cavity cut out was attached to a plastic Petri dish using silicone sealant and capped with a vinyl microslide to make a viewing chamber. The viewing chamber was filled with cell suspension, and placed on the heated stage (≈ 37°C) of an inverted optical microscope (Nikon Eclipse TE300; see Fig. 3 bottom). Micropipettes coated with soluble P-selectin or BSA were inserted into open end of the viewing chamber and connected to a custom-built manometer to control hydrostatic pressure differences between the inside of the micropipette and the viewing chamber. When the micropipette was inserted into the viewing chamber, pressures difference between the micropipette inside and outside was applied. An RBC was aspirated into the micropipette to ensure that there was no RBC motion (and hence no residual pressure) when the manometer was set to zero. This RBC check was repeated between each run with a WBC. An HL-60 cell or neutrophil was aspirated and a pressure difference of 1 to 8 mm of H_2O (9.81 Pa to 78.5 Pa) was applied. Cell motion was observed over a ~160 µm-wide field of view. A video camera attached to the microscope sent images to a video cassette recorder (Sony SVO-9500MD). Images were captured to PC using Labview IMAQ software (National Instruments). If a cell remained stationary for more than 5 or 10 min after initial motion, the cell was discarded.

Analysis of Cell Motion

The positions of the leading and trailing edges of cell were measured as a function of time. Velocity was calculated by dividing the displacement of the cell centroid by the time interval between images. The velocity of cells in BSA-coated micropipettes was tested as a control on every experiment

RESULTS AND DISCUSSION

Adhesion of HL-60 Cells

The first experiments to test adhesion in the micropipette used HL-60 cells [48, 49]. This cell line is frequently used as a model for WBC in other adhesion assays and the cells have been well characterized. A single HL-60 cell was rapidly aspirated into a micropipette and exposed to a pressure difference of 29.4 Pa or 58.8 Pa (values that match those thought be present across short segments in the alveolar capillary bed [12, 13]). It was found that many cells would move for a short while and then stop. Some then resumed moving at hydrodynamic velocity before either stopping again (possibly multiple times) or exiting the field of view. The motion was characterized in terms of 1) the percentage of cells that exhibited an arrest and 2) the average pause time for the arrests that were observed. The percentage of cells that arrested was much larger in soluble P-selectin (sP-s)-coated micropipettes than in BSA-coated micropipettes, but there was no difference in percentage of cells arrested for the two concentrations (0.2 µg/ml and 0.6 µg/ml) of soluble P-selectin used. Increasing the pressure drop across the cell caused a small decrease in percentage of cells arrested.

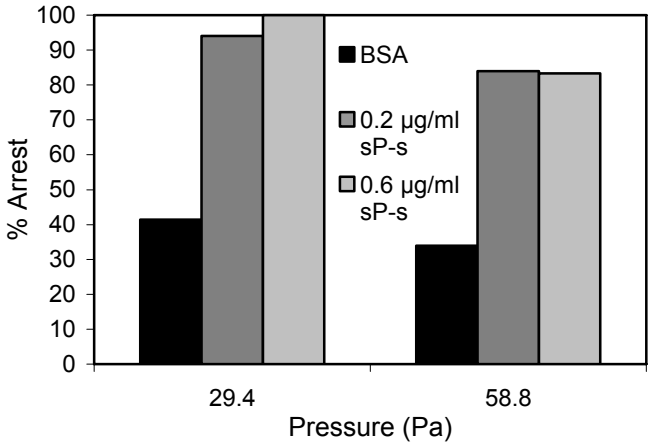

Figure 4. Percentage of HL-60 cells that arrested in 7.8 ± 0.3 µm-ID micropipettes coated with two concentrations of soluble P-selectin (sP-s). Reproduced with permission from [49].

Comparison with parallel plate flow chamber

The micropipette arrest results were compared with adhesion in parallel plate flow chamber assays performed in the laboratory of D. J. Goetz at Ohio University. The bottom surface of a parallel plate flow chamber (Fig. 2B) was coated with the same concentrations of soluble P-selectin as for the micropipette assays. ELISA tests showed that the concentrations on the surface of the micropipette and the parallel plate flow chamber were comparable. HL-60 cells rolled over the P-selectin coated on the bottom surface of the parallel plate flow chamber. A few cells did arrest firmly, but (see Fig. 5) only a tiny percentage compared to the micropipette assay (Fig. 4). These experiments show that HL-60 cells arrest firmly in the micropipette geometry, but not in the parallel plate geometry.

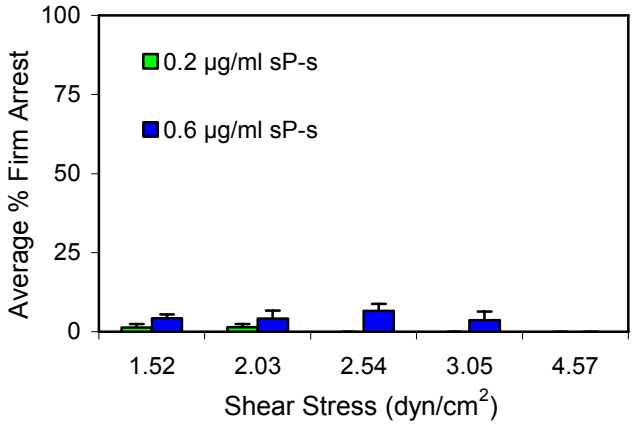

Figure 5. Percentage of HL-60 cells that were firmly arrested on two different coating concentrations of soluble P-selectin in the parallel plate flow chamber. Error bars show SEM. Reproduced with permission from [49].

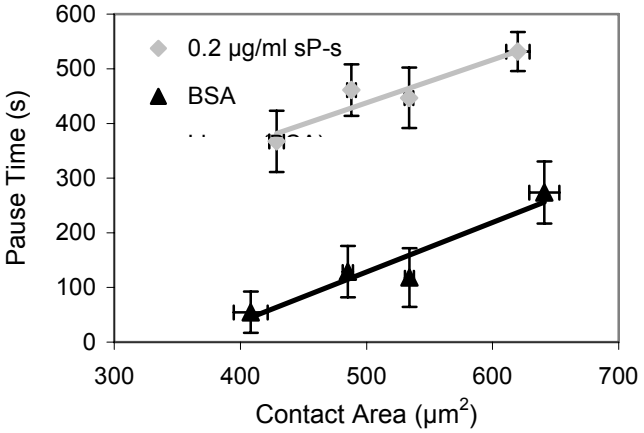

Figure 6. HL-60 pause time as a function of contact area. Data have been averaged in contact area ranges that have approximately equal numbers of cells in each point. Error bars show SEM. Reproduced with permission from [49].

The major geometrical difference between the micropipette assay and the parallel plate flow chamber is the difference in contact area. For the micropipette assay, it was possible to test this further since a range of HL-60 cell diameters (13.5 ± 0.8 µm) and micropipette tip diameters (7.8 ± 0.3 µm) were used. A range of deformation ratios and contact areas (from Eq. 8) was thus accessible. As shown in Fig. 6, the average pause time for HL-60 cells was a function of contact area for both BSA and 0.2 µg/ml soluble P-selectin. The pause times in soluble P-selectin-coated micropipettes were much longer than in BSA-coated micropipettes. This shows that the contact area does play a role in adhesion for the capillary geometry.

Neutrophil exhibit a creeping motion in micropipettes

The HL-60 cells used for initial experiments were a model for WBC, but they are leukemia-associated cancer cells that are larger then normal WBC and may have substantially different mechanical properties. It was necessary to repeat the experiments with normal human WBC. There are many kinds of WBC, but the most prevalent type is the neutrophil. Human neutrophils were isolated from small samples of whole blood from healthy volunteers. Neutrophils were found to behave differently from HL-60 cells. Instead of moving at the velocity of unbound cells and stopping completely, a cell exhibits a continuous creeping motion (Fig. 7 shows a sample) that is much slower than the motion in BSA-coated micropipettes. The distance traveled was tracked every 1 or 2 sec.

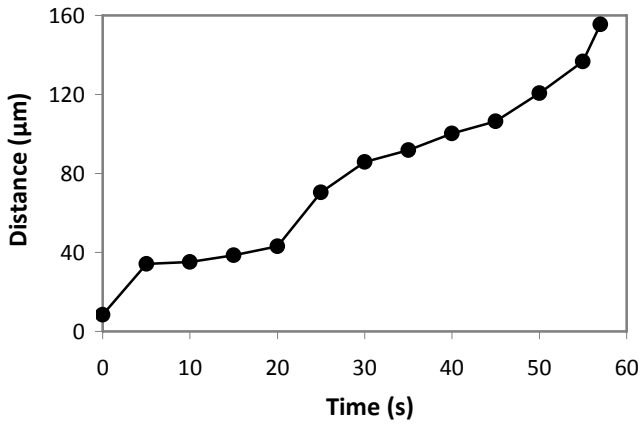

Figure 7. Sample position vs time plot for a creeping neutrophil in a 7.27 µm diameter micropipette coated with 100 µg/ml of soluble P-selectin-coated micropipette, exposed to a pressure of 58.8 Pa.

The creeping velocity for neutrophils moving in micropipettes with an average inner diameter of 6.80 ± 0.27 (SD) µm, coated with 1, 10, 20, 50, or 100 µg/ml soluble P-selectin was compared with that in BSA-coated micropipettes. As shown in Fig. 7, neutrophil creeping velocity varies slightly as the cell travels down the micropipette. The average velocity, U, for each track was determined. Equation 4 shows that U/R_p that scales with pressure so the average velocity was divided by R_p for that track to compute U/R_p for a track. The average of the $<U/R_p>$ was computed by averaging all tracks. This $<U/R_p>$ is shown in Fig. 8 as a function of pressure difference. Pressure differences similar to physiological values across a single pulmonary capillary segment (10 - 80 Pa) were applied to the

micropipettes: 1, 2, 3, 4, 6, and 8 mm of water (9.8 - 78.5 Pa). Neutrophil velocities in all concentrations of soluble P-selectin-coated microvessels were slower than in BSA-coated microvessels for each of the pressure differences. Neutrophil velocity increases linearly as the pressure difference increases for all concentrations of sP-selectin, as expected from Eq. 4.

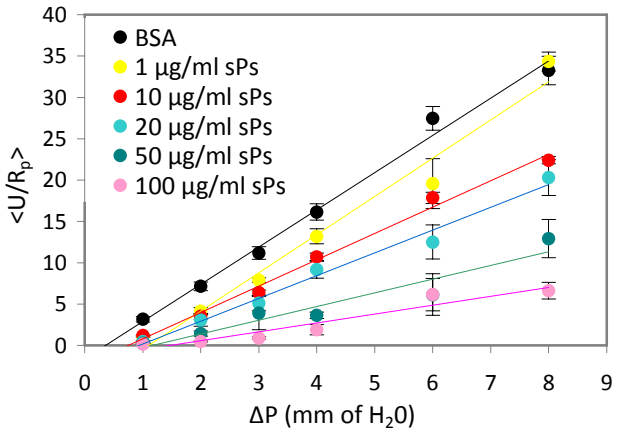

Figure 8. Average U/R_p vs pressure difference for neutrophils moving in micropipettes coated with BSA or a variety of concentrations of soluble P-selectin. Error bars show SEM.

As noted from Eq. 4, the x-axis intercept is proportional to the external force (due to bonds), which (with the exception of the lowest concentration) increases with increasing concentration of soluble P-selectin. The slope of the lines decreases with increasing concentration of soluble P-selectin. This suggests that the gap difference also changes as the number of bonds increases.

Creeping Mechanism

There are at least 3 mechanisms for the creeping behavior. Two are illustrated graphically below. All mechanisms assume that the slow motion is mediated by bonds. Equation 4 shows that if the force on a cell is known then the velocity is known, but because the bonds between the cell and the surface are likely to be relatively few in number and to form and break dynamically, there are likely to be variations in the velocity.

1) Complete bond breakage model: For this model (shown in Fig. 9), the cell is held in place ($U = 0$) by a small number of bonds. These bonds all become equally stretched. The stretching increases the rate of breakup so that all bonds rupture in a short time. The cell can then move at the free velocity, U_f before it arrests again due to bond formation. If bond dissociation is fast and bond association relatively slow (here, δx_1 depends on the bond association rate), then this mechanism can produce velocities comparable to those seen. The variance in velocity, however, will be large on the timescale of association since the motion is, essentially, stop-start.

2) Centipede Model: This model (shown in Fig. 10) is based on continuous stochastic breakage of stressed bonds. The model assumes that as the cell moves, some bonds become stretched.

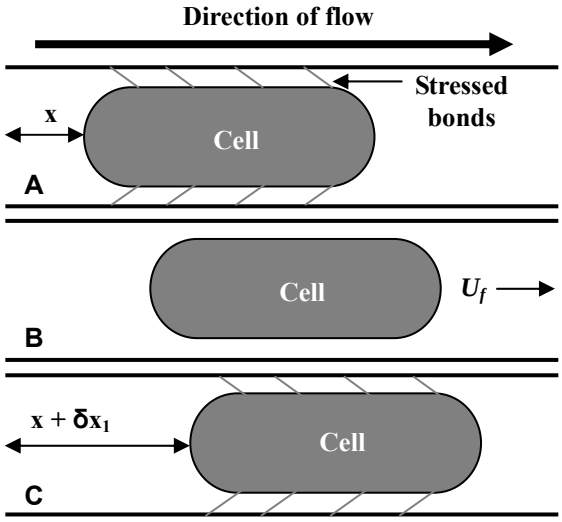

Figure 9. Complete bond breakage model. A) A small number of bonds have formed between the cell and the vessel wall, resulting in cell arrest. B) Bonds have all broken and the cell can move at the free flow velocity, U_f. This segment ends when bonds form again at C).

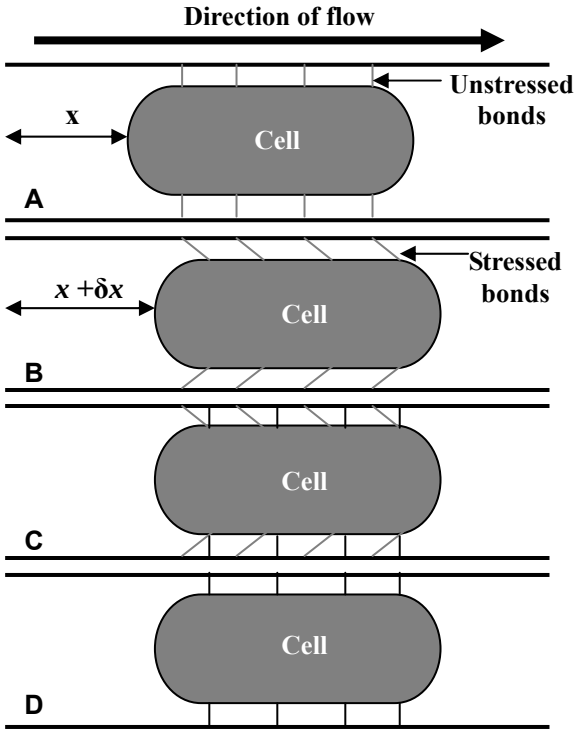

Figure 10. Centipede model. A) Bonds form between the cell and vessel wall. B) Bonds are stretched by cell motion. C) New, unstretched bonds form. D) The stretched bonds rupture leaving only the unstretched bonds. The cycle can then repeat.

The bond association rate, however, is large enough that before those initial bonds break, other bonds form in an

unstretched position. Stretched bonds experience a force that causes the bonds to break more quickly so those initial bonds eventually break, leaving the formerly unstretched bonds behind. Those bonds can then elongate and become stretched in turn. In this model, there are always some bonds between the cell and vessel wall. One can estimate the velocity in this model by estimating the step size δx ~ size of P-selectin-ligand bonds ~ 50 nm and the time step, δt ~ stressed lifetime of bonds ~ 0.2 s, so the velocity $v \sim \delta x/\delta t$ = 250 nm/s. This is consistent with some of the cell velocities observed.

3) Tank Tread Model of Creeping (not illustrated): If only a small number of bonds form between the cell and surface, then it is likely that there will be an unbalanced torque on the cell due to bonds. Although the cell is constrained to keep a capsule shape by the tube geometry, since the cell is deformable, membrane should be able to flow around the bonds to balance the torque. That could result in a creeping motion as well.

Simulations to determine which of these models best fits the neutrophil velocity and velocity variance are ongoing.

Activation and Cyclic Migratory behavior: In performing the initial experiments on human neutrophil motion in micropipettes, an interesting new phenomenon was observed [50]. Micropipette tips with ID 6.53 ± 0.10 (SD) μm were coated with either BSA or 0.6 μg/ml of soluble P-selectin according to the same protocol which was used in HL-60 cell studies and neutrophils were exposed to a pressure difference of 29.4 Pa. It was found that neutrophils that arrested in pulmonary capillary-sized glass microvessels coated with either BSA or 0.6 μg/ml of P-selectin were often observed to exhibit a 'Cyclic Migratory Behavior' (CMB). An example of CMB is shown in Fig. 11. The neutrophil is seen to crawl against the pressure gradient to the mouth of the micropipette where it is subsequently reaspirated and brought back into the micropipette. This behavior can recur for several cycles.

The fraction of cells that exhibited CMB in 0.6 μg/ml P-selectin-coated micropipettes (55%) was almost twice the fraction seen in BSA-coated micropipettes. CMB only began after several minutes had elapsed, but there was no significant difference in time to start CMB between BSA and 0.6 μg/ml P-selectin-coated micropipettes) [50].

The biochemical and biophysical mechanism responsible for this behavior is the subject of current investigation. It was found that CMB could be eliminated if the BSA used to block the micropipettes was heat treated at 50°C for 2 hours in a water bath before blocking. If the same heat treated BSA was kept at 4°C overnight and used to block the microvessel surface, the CMB returned. It seems that there is something in BSA which mediated CMB.

It has been observed *in vivo* that following arrest of WBC in the microvasculature, the ligation of L-selectin or β_2 integrins initiates a signaling pathway which causes the neutrophils to flatten and crawl preferentially towards sites where they can pass through the vessel wall [4, 51]. It has also been suggested that the crawling is mediated by integrins or some other unknown molecules [51, 52]. The signaling induced by ligation of ECAMs is also known to cause spacially inhomogeneous cytoskeletal reorganization in neutrophils [51] that contribute to the crawling and migration of cell [51, 53, 54].

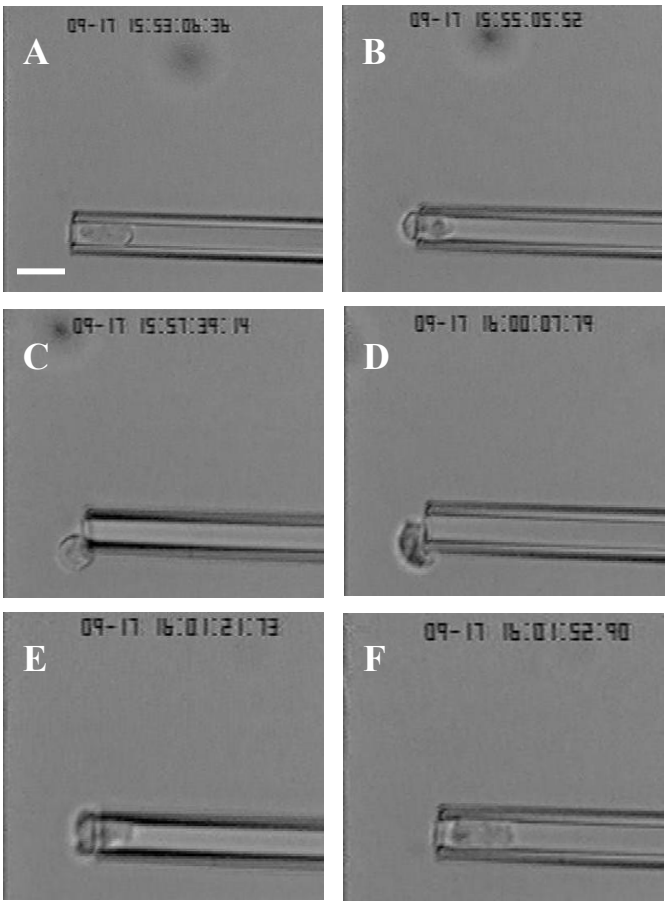

Figure 11. Cyclic Migratory Behavior. A) Capsule-shaped neutrophil arrested in a micropipette (ID ~6.5 μm) coated with 0.6 μg/ml soluble P-selectin with a ΔP = 29.4 Pa. B) Neutrophil starts to crawl out of the microvessel. C) Neutrophil is completely outside and has mostly recovered its original spherical shape. D) Neutrophil starts to spread at the mouth of microvessel. E) Neutrophil starts to re-aspirate into the microvessel. F) Neutrophil is completely inside the microvessel and has again deformed into a capsule shape. This completes one cycle of the Cyclic Migratory Behavior. Bar is 10 μm.

Microrheology for Regional Rheological Properties

In work done by Masters student Anand Pai [55], the motion of granules inside aspirated neutrophils was tracked at 60x magnification and Differential Interference Contrast. From the Brownian motion of the granules one can calculate the shear and elastic moduli for the region in which the granules are located. As shown in Fig. 12, it was found that the body region was modestly stiffer than the lead or trail regions and the elastic moduli in all regions increased significantly when cells were aspirated into ICAM-1-coated micropipettes compared to BSA-coated micropipettes.

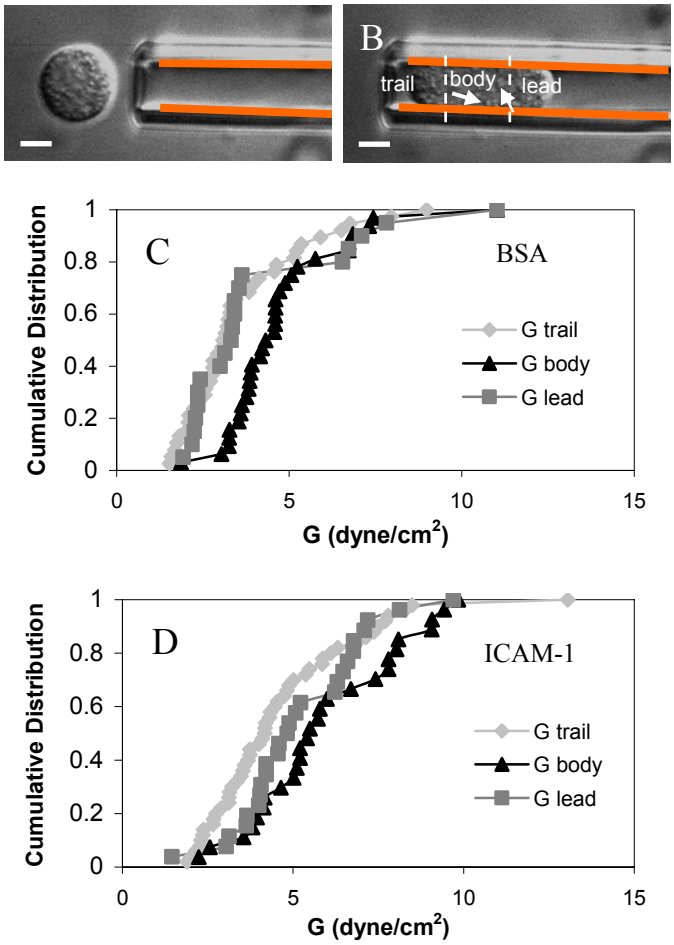

Figure 12. Tracking of granules inside neutrophils aspirated into a micropipette. A) Neutrophil before aspiration. B) Neutrophil following aspiration. Arrows show granules. Lead, body and trail regions are indicated. Scale bar = 5 µm. C) Cumulative distribution of viscoelastic moduli for granules in the lead body and trail regions for cell aspirated into BSA-coated micropipettes. D) Cumulative distribution of viscoelastic moduli for granules in the lead body and trail regions for cell aspirated into ICAM-1-coated micropipettes. Reproduced with permission from [55].

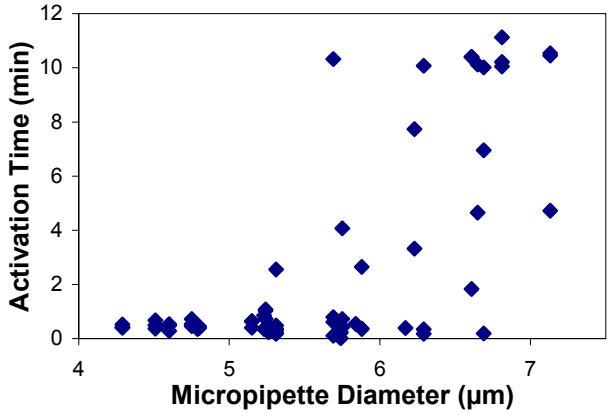

Figure 13. Graph of Activation time vs micropipette diameter for neutrophils aspirated into BSA-coated micropipettes.

Aspiration-induced Mechanical Activation

It was also found that cells would activate in small micropipettes. After a time lag following activation, the cell would begin to put out pseudopods and begin to move. As shown in Fig. 13, the smaller the micropipette the faster the neutrophils became activated. One activated, the neutrophil would start migrating. This effect is the subject of ongoing investigations including more accurately determining the moment of activation in the micropipette by observing the flux of Calcium that is expected to accompany it.

CONCLUSIONS

The work with HL-60 cell shows that there can be cell arrest and pausing mediated by P-selectins for large cell deformation ratios in the capillary geometry. In addition, the HL-60 cells adhere more strongly to similar concentrations of selectin in the micropipette than in parallel plate flow chambers where the contact area is much larger. The pause times for HL-60 cells increase with increasing area of contact in micropipettes.

For human neutrophils, which are much smaller than HL-60 cells and hence suffer less deformation upon aspiration, a different creeping type of adhesion was seen which is dependent on P-selectin but not ICAM-1. The mechanism for this creeping motion is the subject of further investigations.

Even though adhesion in P-selectin-coated micropipettes is much greater than for BSA-coated micropipettes, for both neutrophils and HL-60 cells the adhesion to P-selectin has proved to be difficult to completely block with antibodies in this geometry. This could explain some of the null results seen for blocking antibodies against selectins in vivo.

Microrheological experiments show that there are modest regional differences in internal rheological parameters following aspiration and the cells stiffen on exposure to ICAM-1. This could be relevant to ICAM-1 mediated arrest. In addition, as shown by others, neutrophils can become mechanically activated upon aspiration into small micropipettes. The activation time is longer for larger micropipettes but shortens substantially for micropipettes smaller than 5.5 µm.

ACKNOWLEDGMENTS

The authors wish to thank Xiaoyan Zou for help with the parallel plate flow chamber work. This work was supported by an award from the American Heart Association and by grant BES-0547165 from the National Science Foundation.

REFERENCES

[1] Andonegui, G., Bonder, C. S., Green, F., Mullaly, S. C., Zbytnuik, L., Raharjo, E., and Kubes, P., 2003, "Endothelium-Derived Toll-Like Receptor-4 Is the Key Molecule in Lps-Induced Neutrophil Sequestration into Lungs," J. Clin. Invest, **111**(7), pp. 1011-1020.

[2] Erzurum, S. C., Downey, G. P., Doherty, D. E., Schwab III, B., Elson, E. L., and Worthen, G. S., 1992, "Mechanisms of

Lipopolysaccharide-Induced Neutrophil Retention: Relative Contributions of Adhesive and Cellular Mechanical Properties," J. Immunol, **149**(1), pp. 154-162.
[3] Gebb, S. A., Graham, J. A., Hanger, C. C., Godbey, P. S., Capen, R. L., Doerschuk, C. M., and Wagner Jr, W. W., 1995, "Sites of Leukocyte Sequestration in the Pulmonary Microcirculation," J. Appl. Physiol, **79**(2), pp. 493-497.
[4] Burns, A. R., Smith, C. W., and Walker, D. C., 2003, "Unique Structural Features That Influence Neutrophil Emigration into the Lung," Physiol. Rev, **83**(2), pp. 309-336.
[5] Doerschuk, C. M., Winn, R. K., Coxson, H. O., and Harlan, J. M., 1990, "Cd18-Dependent and -Independent Mechanisms of Neutrophil Emigration in the Pulmonary and Systemic Microcirculation of Rabbits," J. Immunol, **144**(6), pp. 2327-2333.
[6] Doyle, N. A., Bhagwan, S. D., Meek, B. B., Kutkoski, G. J., Steeber, D. A., Tedder, T. F., and Doerschuk, C. M., 1997, "Neutrophil Margination, Sequestration, and Emigration in the Lungs of L-Selectin-Deficient Mice," J. Clin. Invest, **99**(3), pp. 526-533.
[7] Kubo, H., Doyle, N. A., Graham, L., Bhagwan, S. D., Quinlan, W. M., and Doerschuk, C. M., 1999, "L- and P-Selectin and Cd11/Cd18 in Intracapillary Neutrophil Sequestration in Rabbit Lungs," Am. J. Respir. Crit. Care Med, **159**(1), pp. 267-274.
[8] Doerschuk, C. M., Beyers, N., Coxson, H. O., Wiggs, B., and Hogg, J. C., 1993, "Comparison of Neutrophil and Capillary Diameters and Their Relation to Neutrophil Sequestration in the Lung," J. Appl. Physiol, **74**(6), pp. 3040-3045.
[9] Shao, J. Y. and Hochmuth, R. M., 1997, "The Resistance to Flow of Individual Human Neutrophils in Glass Capillary Tubes with Diameters between 4.65 and 7.75 Mm," Microcirc, **4**(1), pp. 61-74.
[10] Sobin, S. S. and Fung, Y. C., 1992, "Response to Challenge to the Sobin-Fung Approach to the Study of Pulmonary Microcirculation," Chest, **101**(4), pp. 1135-1143.
[11] Guntheroth, W. G., Luchtel, D. L., and Kawabori, I., 1982, "Pulmonary Microcirculation: Tubules Rather Than Sheet and Post," J. Appl. Physiol, **53**(2), pp. 510-515.
[12] Bathe, M., Shirai, A., Doerschuk, C. M., and Kamm, R. D., 2002, "Neutrophil Transit Times through Pulmonary Capillaries: The Effects of Capillary Geometry and Fmlp-Stimulation," Biophys. J, **83**(4), pp. 1917-1933.
[13] Huang, Y., Doerschuk, C. M., and Kamm, R. D., 2001, "Computational Modeling of Rbc and Neutrophil Transit through the Pulmonary Capillaries," J. Appl. Physiol, **90**, pp. 545-564.
[14] Abraham, E., 2003, "Neutrophils and Acute Lung Injury," Crit Care Med, **31**, pp. S195-199.
[15] Matthay, M. A. and Zimmerman, G. A., 2005, "Acute Lung Injury and the Acute Respiratory Distress Syndrome: Four Decades of Inquiry into Pathogenesis and Rational Management.," Am. J. Respir. Cell Mol. Biol., **33**(4), pp. 319-327.
[16] Mulligan, M. S., Polley, M. J., Bayer, R. J., Nunn, M. F., Paulson, J. C., and Ward, P. A., 1992, "Neutrophil-Dependent Acute Lung Injury. Requirement for P-Selectin (Gmp-140)," J. Clin. Invest, **90**(4), pp. 1600–1607.
[17] Reutershan, J., Basit, A., Galkina, E. V., and Ley, K., 2005, "Sequential Recruitment of Neutrophils into Lung and Bronchoalveolar Lavage Fluid in Lps-Induced Acute Lung Injury," Am. J. Physiol. Lung Cell. Mol. Physiol., **289**(5), pp. L807-L815.
[18] Riedemann, N. C., Guo, R. F., Hollmann, T. J., Gao, H., Neff, T. A., Reuben, J. S., Speyer, C. L., Sarma, J. V., Wetsel, R. A., Zetoune, F. S., and Ward, P. A., 2004, "Regulatory Role of C5a in Lps-Induced Il-6 Production by Neutrophils During Sepsis," FASEB J., **18**, pp. 370-372.
[19] Riedemann, N. C., Guo, R.-F., and Ward, P. A., 2003, "The Enigma of Sepsis," J. Clin. Invest, **112**(4), pp. 460-467.
[20] Ward, P. A. and Hunninghake, G. W., 1998, "Lung Inflammation and Fibrosis," Am J Respir Crit Care Med, **157**, pp. S123-129.
[21] Fuhlbrigge, R. C., Alon, R., Puri, K. D., Lowe, J. B., and Springer, T. A., 1996, "Sialylated, Fucosylated Ligands for L-Selectin Expressed on Leukocytes Mediate Tethering and Rolling Adhesions in Physiologic Flow Conditions," J. Cell Biol, **135**(3), pp. 837-848.
[22] Puri, K. D., Finger, E. B., and Springer, T. A., 1997, "The Faster Kinetics of L-Selectin Than of E-Selectin and P-Selectin Rolling at Comparable Binding Strength," J. Immunol, **158**, pp. 405-413.
[23] Lawrence, M. B. and Springer, T. A., 1993, "Neutrophils Roll on E-Selectin," J. Immunol, **151**(11), pp. 6338-6346.
[24] Alon, R., Chen, S., Fuhlbrigge, R., Puri, K. D., and Springer, T. A., 1998, "The Kinetics and Shear Threshold of Transient and Rolling Interactions of L-Selectin with Its Ligand on Leukocytes," Proc. Natl. Acad. Sci. USA, **95**, pp. 11631-11636.
[25] Lawrence, M. B. and Springer, T. A., 1991, "Leukocytes Roll on a Selectin at Physiological Flow Rates: Distinction from and Prerequisite for Adhesion through Integrins," Cell, **65**, pp. 859-874.
[26] Kukreti, S., Smith, C. W., and McIntire, L. V., 1995, "Role of P-Selectin in Histamine Induced Monocyte Rolling on Endothelial Cells," Biorheology, **32**, pp. 141.
[27] Jones, D. A., Abbassi, O., McIntire, L. V., McEver, R. P., and Smith, C. W., 1993, "P-Selectin Mediates Neutrophil Rolling on Histamine Stimulated Endothelial Cells," Biophys. J, **65**(4), pp. 1560-1569.
[28] Abbassi, O., Kishimoto, T. K., McIntire, L. V., Anderson, D. C., and Smith, C. W., 1993, "E-Selectin Supports Neutrophil Rolling *in Vitro* under Conditions of Flow," J. Clin. Invest, **92**, pp. 2719-2730.
[29] Ley, K. and Gaehtgens, P., 1991, "Endothelial, Not Hemodynamic, Differences Are Responsible for Preferential Leukocyte Rolling in Rat Mesenteric Venules," Circ. Res, **69**(4), pp. 1034-1041.

[30] Borges, E., Eytner, R., Moll, T., Steegmaier, M., Campbell, M. A., Ley, K., Mossmann, H., and Vestweber, D., 1997, "The P-Selectin Glycoprotein Ligand-1 Is Important for Recruitment of Neutrophils into Inflamed Mouse Peritoneum," Blood, **90**(5), pp. 1934-1942.
[31] Kunkel, E. J., Dunne, J. L., and Ley, K., 2000, "Leukocyte Arrest During Cytokine-Dependent Inflammation in Vivo," J. Immunol, **164**, pp. 3301-3308.
[32] Springer, T. A., 1990, "Adhesion Receptors of the Immune System," Nature (London), **346**, pp. 425-434.
[33] Kansas, G. S., 1996, "Selectins and Their Ligands: Current Concepts and Controversies," Blood, **88**(9), pp. 3259-3287.
[34] Varki, A., 1994, "Selectin Ligands," Proc. Natl. Acad. Sci. USA, **91**, pp. 7390-7397.
[35] Varki, A., 1997, "Selectin Ligands: Will the Real Ones Please Stand Up?," J. Clin. Invest, **99**(2), pp. 158-162.
[36] Springer, T. A., 1994, "Traffic Signals for Lymphocyte Recirculation and Leukocyte Emigration: The Multistep Paradigm," Cell, **76**, pp. 301-314.
[37] Kuebler, W. M., Kuhnle, G. E. H., Groh, J., and Goetz, A. E., 1997, "Contribution of Selectins to Leucocyte Sequestration in Pulmonary Microvessels by Intravital Microscopy in Rabbits," J. Physiol.-London, **501**(2), pp. 375-386.
[38] Shao, J.-Y. and Hochmuth, R. M., 1996, "Micropipette Suction for Measuring Piconewton Forces of Adhesion and Tether Formation from Neutrophil Membranes," Biophys. J, **71**(5), pp. 2892-2901.
[39] Yeung, A. and Evans, E., 1989, "Cortical Shell-Liquid Core Model for Passive Flow of Liquid-Like Spherical Cells into Micropipets," Biophys. J, **56**(1), pp. 139-149.
[40] Evans, E. and Rawicz, W., 1990, "Entropy-Driven Tension and Bending Elasticity in Condensed-Fluid Membranes," Phys. Rev. Lett, **64**(17), pp. 2094-2097.
[41] Evans, E. A., 1989, "Structure and Deformation Properties of Red Blood Cells: Concepts and Quantitative Methods," Methods Enzymol, **173**, pp. 3-35.
[42] Tsai, M. A., Frank, R. S., and Waugh, R. E., 1993, "Passive Mechanical Behavior of Human Neutrophils: Power-Law Fluid," Biophys. J, **65**(5), pp. 2078-2088.
[43] Berk, D. A. and Hochmuth, R. M., 1992, "Lateral Mobility of Integral Proteins in Red Blood Cell Tethers," Biophys. J, **61**(1), pp. 9-18.
[44] Harris, A. G. and Skalak, T. C., 1993, "Effects of Leukocyte Activation on Capillary Hemodynamics in Skeletal-Muscle," Am. J. Physiol, **264**(3), pp. H909-H916.
[45] Bagge, U., Skalak, R., and Attefors, R., 1977, "Granulocyte Rheology: Experimental Studies in an in-Vitro Microflow System," Adv. Microcirc., **7**, pp. 29-48.
[46] Tran-Son-Tay, R., Kirk III, T. F., Zhelev, D. V., and Hochmuth, R. M., 1994, "Numerical Simulation of the Flow of Highly Viscous Drops Down a Tapered Tube," J. Biomech. Eng, **116**, pp. 172-176.
[47] Goetz, D. J., Ding, H., Atkinson, W. J., Vachino, G., Camphausen, R. T., Cumming, D. A., and Luscinskas, F. W., 1996, "A Human Colon Carcinoma Cell Line Exhibits Adhesive Interactions with P-Selectin under Fluid Flow Via a Psgl-1- Independent Mechanism," Am. J. Pathol, **149**(5), pp. 1661-1673.
[48] Tees, D. F. J., Sundd, P., and Goetz, D. J., 2006, "A Flow Chamber for Capillary Networks: Leukocyte Adhesion in Capillary-Sized, Ligand-Coated Micropipettes," in *Principles of Cellular Engineering: Understanding the Biomolecular Interface*, M. R. King, Editor. Academic Press: New York, pp. 213-231.
[49] Sundd, P., Zou, X., Goetz, D. J., and Tees, D. F. J., 2008, "Leukocyte Adhesion in Capillary-Sized, P-Selectin-Coated Micropipettes," Microcirc, **15**(2), pp. 109-122.
[50] Sundd, P., 2007, "Micropipette Cell Adhesion Assay: A Novel in Vitro Assay to Model Leukocyte Adhesion in the Pulmonary Capillaries of the Lung," Ph.D. thesis, Ohio University, Athens, OH.
[51] Doerschuk, C. M., 2001, "Mechanisms of Leukocyte Sequestration in Inflamed Lungs," Microcirc, **8**(2), pp. 71-88.
[52] Malawista, S. E. and de Boisfleury Chevance, A., 1997, "Random Locomotion and Chemotaxis of Human Blood Polymorphonuclear Leukocytes (Pmn) in the Presence of Edta: Pmn in Close Quarters Require Neither Leukocyte Integrins nor External Divalent Cations," Proc. Natl. Acad. Sci. USA, **94**, pp. 11577-11582.
[53] Gaborski, T. R. and McGrath, J. L., 2006, "Dynamics of the Neutrophil Surface During Emigration from Blood," in *Principles of Cellular Engineering: Understanding the Biomolecular Interface*, M. R. King, Editor. Academic Press: New York, pp. 123-142.
[54] Moazzam, F., DeLano, F. A., Zweifach, B. W., and Schmid-Schönbein, G. W., 1997, "The Leukocyte Response to Fluid Stress," Proc. Natl. Acad. Sci. USA, **94**, pp. 5338-5343.
[55] Pai, A., Sundd, P., and Tees, D. F. J., 2008, "In Situ Microrheological Determination of Neutrophil Stiffening Following Adhesion in a Model Capillary," Ann. Biomed. Eng, **36**(4), pp. 596-603.

